Proceedings of the Sixteenth International Conference on
Computational Structures Technology
Edited by: P. Iványi, J. Kruis and B.H.V. Topping
Civil-Comp Conferences, Volume 14, Paper 11.2
Civil-Comp Press, Edinburgh, United Kingdom, 2026
ISSN: 2753-3239, doi: 10.4203/ccc.14.11.2

Coupled Thermo-Mechanical Analysis in Excavation Damage Zone

J. Kruis, T. Krejci and T. Koudelka

Faculty of Civil Engineering, Czech Technical University in Prague, Czechia

Abstract

Deep geological repositories for radioactive waste are usually planned in crystalline rocks which are brittle and contain fractures of various scales. The fractures can create preferential paths for transport of water which may contain various chemical species or radionuclides. It is therefore essential to know how much of the substance would reach the rock mass in the event of an accident. If the engineering barrier is capable of containing any potential leakage of hazardous substances, the excavation damage zone is not a critical factor in the safety assessment. This contribution therefore focuses on a detailed analysis of the behaviour of a single borehole and its impact on the surrounding environment. For transport processes and related safety assessment of deep geological repositories is crucial to describe the amount of any transported species close to the rock mass. Results from such analysis will serve in detailed study of excavation damage zone. To provide an accurate description of the repository, the model must also include engineering barriers, which are usually made of bentonite. The behaviour of bentonite is highly complex, and a specialised material model must be used to describe it. All analyses are based on the finite element method. The nonlinear behaviour is solved with the help of the Newton's method and time integration is done by the generalized trapezoidal rule.

Keywords: excavation damage zone, damage model, thermo-mechanical analysis, generalized trapezoidal rule, coupled modeling, fem.

1 Introduction

The issue of deep geological repositories is being addressed by a large number of research teams, and major European projects such as BEACON and EURAD [5] are dedicated to this field. This is because extremely high safety requirements are placed on these repositories. It is necessary to verify all possible scenarios regarding the behaviour and loading of the repositories, which leads to a large number of numerical analyses.

Spent nuclear fuel generates heat, and it is therefore necessary to design the storage galleries and boreholes in such a way that the temperature remains below 95 °C at all times; this value is derived with regard to the corrosion of the waste disposal packages and also ensures that the water does not boil.

Another significant problem is the sealing of the waste disposal packages using bentonite. Bentonite is a clay-like soil capable of absorbing large amount of water whilst increasing in volume. This ensures that all voids are filled and that swelling pressure increases. This pressure must be adjusted so as to prevent the waste disposal package from losing stability.

2 Hypoplastic model of bentonite

In this contribution, the behaviour of bentonite is described using a hypoplastic model proposed by Mašín [1] and [2]. The effective stress rate of the macrostructure incorporating suction and saturation degrees is defined in the form

$$\dot{\boldsymbol{\sigma}}_M = f_s \left(\boldsymbol{L} : (\dot{\boldsymbol{\varepsilon}} - f_m \dot{\boldsymbol{\varepsilon}}_m) + f_d \boldsymbol{N} \| \dot{\boldsymbol{\varepsilon}} - f_m \dot{\boldsymbol{\varepsilon}}_m \| \right) + f_u (\boldsymbol{H}_s + \boldsymbol{H}_T) \tag{1}$$

where $\dot{\varepsilon}$ denote the macrostructural strain rate, $\dot{\varepsilon}_m$ denote the microstructural strain rate, f_s is the scalar function controlling barotropy, f_d is the scalar function controlling pyknotropy (stiffness reduction with deformation), f_u is the scalar function controlling structural collapse, $\boldsymbol{L}$ is the constitutive tensor governing mechanical stiffness, $\boldsymbol{N}$ is the constitutive tensor governing deformation anisotropy, $\boldsymbol{H}_s$ represents vector accounting for collapse mechanisms induced by wetting, $\boldsymbol{H}_T$ represents vector accounting for collapse mechanisms induced by heating.

3 Governing equations

The coupled heat and moisture transfer in deforming porous media such as soils can be successfully described by a micromechanical-based model presented in [4]. This approach uses an averaging process assuming that dry air, vapor, and moist air occupy the same volume fraction in the volume together with the solid phase and the liquid water. Three primary unknowns are defined in the material point - pore water pressure, p^w, pore gas pressure, p^g, and temperature, T for the transport part. Generally, three unknown displacements u, v, w are defined for the mechanical part. A choice of primary unknowns with pore capillary pressure, p^c, instead of pore water pressure, p^w, is recommended in literature dealing with the modeling of concrete and soils loaded by high temperatures.

The moist air in the pore system is usually assumed to be a perfect mixture of two ideal gases dry air and water vapor. In soils, the water is usually present as a condensed liquid that is separated from its vapor by a concave meniscus (capillary water) because of the surface tension. The capillary pressure is defined as the pressure difference between the gas phase and the liquid phase, by the capillary pressure equation

$$p^c = p^g - p^w \ . \tag{2}$$

The moisture retention curve is an alternative representation of the pore size distribution. It demonstrates the connection between the suction stress, s, and the water accumulated. The suction stress rapidly decreases from the upward hygroscopic moisture as the large pores are filled with water. In soil mechanics [4], the moisture retention curves are mostly substituted by the material relationship between capillary pressure p^c, saturation degree S_w and temperature T

$$p^c = p^c(S_w, T). \tag{3}$$

In the case of expansive soils, the volume changes are significant phenomena influencing also the capability of absorbing moisture from an environment. The degree of saturation S_w depends on suction stress s, void ratio, and the suction-loading path. The previous relationship can be expressed in an inverse form with the dependence on the mentioned volume changes

$$S_w = S_w(p^c, T, \varepsilon_V), \tag{4}$$

where ε_V is the volume strain measured from a reference state.

The final form of the governing equations is obtained by the introduction of transport equations, i.e. Darcy's law and Fick's law into the mass balance equations for dry air and water species together with an assumption of slow phenomena with inertia forces neglected. Assuming small displacements and heat and moisture fluxes related to the solid phase, material derivatives $\mathrm{D}^s/\mathrm{D}t$ can be replaced by the standard time derivatives $\partial/\partial t$. For the expansive soil modeling, the premises of incompressible grains and incompressible water are adopted ($\alpha = 1$, $1/K_s = 0$, and $1/K_w = 0$). It has to be mentioned that saturation degree is also the function of the volume changes, so its derivative reads

$$\frac{\partial S_w}{\partial t} = \frac{\partial S_w}{\partial p^c}\frac{\partial p^g}{\partial t} - \frac{\partial S_w}{\partial p^c}\frac{\partial p^w}{\partial t} + \frac{\partial S_w}{\partial T}\frac{\partial T}{\partial t} + \frac{\partial S_w}{\partial \varepsilon_{\mathrm{V}}}\frac{\partial \varepsilon_{\mathrm{V}}}{\partial t}, \tag{5}$$

where

$$\frac{\partial \varepsilon_{\mathrm{V}}}{\partial t} = \boldsymbol{m}\frac{\partial \boldsymbol{\varepsilon}}{\partial t} = \boldsymbol{m}\boldsymbol{\partial}\frac{\partial \boldsymbol{u}}{\partial t} = \mathrm{div}\boldsymbol{v}^{s}. \tag{6}$$

Note that

$$\frac{\partial S_w}{\partial t} = -\frac{\partial S_g}{\partial t}. \tag{7}$$

The final balance equations are summarized below. Mass balance equation for dry air

$$\begin{aligned} & S_g \mathrm{div}\boldsymbol{v}^s - \beta_s(1-n)S_g\frac{\partial T}{\partial t} - n\frac{\partial S_w}{\partial t} + \frac{nS_g}{\rho^{ga}}\frac{\partial}{\partial t}\left(\frac{M_a}{TR}p^{ga}\right) + \\ & \frac{1}{\rho^{ga}}\mathrm{div}\left[\rho^g\frac{M_aM_w}{M_g^2}\boldsymbol{D}_g\mathrm{grad}\left(\frac{p^{gw}}{p^g}\right)\right] + \frac{1}{\rho^{ga}}\mathrm{div}\left[\frac{k^{rg}\boldsymbol{k}\rho^{ga}}{\mu^g}\left(-\mathrm{grad}p^g + \rho^g\boldsymbol{g}\right)\right] = 0\,. \end{aligned} \tag{8}$$

where S_g is the degree of gas saturation, $\boldsymbol{v}^s$ expresses the mass averaged solid velocity, M_a, M_w and M_g are the molar masses of individual constituents, n is the porosity, T is the temperature, S_w is the degree of water saturation, R is the gas constant, $\boldsymbol{D}_g$ is the effective dispersive tensor, $\boldsymbol{k}$ is the intrinsic permeability tensor, k^{rg} and k^{rw} are the dimensionless relative permeabilities, μ is the dynamic viscosity, $\boldsymbol{g}$ is the gravitational acceleration. ρ^g is the density of moist air, ρ^{ga} is the density of dry air, ρ^{gw} is the density of water vapor. Mass balance equation for water species, i.e. liquid water and water vapor

$$\begin{aligned} & \left(\rho^w S_w + \rho^{gw} S_g\right)\mathrm{div}\boldsymbol{v}^s - \beta_{swg}\frac{\partial T}{\partial t} + \\ + \quad & (\rho^w + \rho^{gw})n\frac{\partial S_w}{\partial t} + nS_g\frac{\partial}{\partial t}\left(\frac{M_w}{TR}p^{gw}\right) + \mathrm{div}\left[-\rho^g\frac{M_aM_w}{M_g^2}\boldsymbol{D}_g\mathrm{grad}\left(\frac{p^{gw}}{p^g}\right)\right] + \\ + \quad & \mathrm{div}\left[\frac{k^{rg}\boldsymbol{k}\rho^{gw}}{\mu^g}\left(-\mathrm{grad}p^g + \rho^g\boldsymbol{g}\right)\right] + \mathrm{div}\left[\frac{k^{rw}\boldsymbol{k}\rho^{w}}{\mu^w}\left(-\mathrm{grad}p^w + \rho^w\boldsymbol{g}\right)\right] = 0\,. \end{aligned} \tag{9}$$

Enthalpy balance equation of the multiphase medium

$$\big(\rho C_p\big)_{\mathrm{eff}}\frac{\partial T}{\partial t} + \big(\rho_w C_p^w\boldsymbol{v}^w + \rho_g C_p^g\boldsymbol{v}^g\big)\cdot\mathrm{grad}T - \mathrm{div}\big(\boldsymbol{\lambda}_{\mathrm{eff}}\mathrm{grad}T\big) = -\dot{m}_{\mathrm{vap}}\Delta H_{\mathrm{vap}}, \tag{10}$$

where $\boldsymbol{\lambda}_{\mathrm{eff}}$ is the effective thermal conductivity tensor, $\dot{m}_{\mathrm{vap}}$ is obtained from mass balance equation for liquid water

$$\dot{m}_{\mathrm{vap}} = -\alpha S_w\rho^w\mathrm{div}\boldsymbol{v}^s + \rho^w\beta_{sw}\frac{\partial^s T}{\partial t} - \rho^w n\frac{\partial^s S_w}{\partial t} - \mathrm{div}(nS_w\rho^w\boldsymbol{v}^{ws}), \tag{11}$$

and convective heat fluxes read

$$\begin{aligned} \rho_w C_p^w\boldsymbol{v}^w &= n\rho^w C_p^w\frac{k^{rw}\boldsymbol{k}\rho^w}{\mu^w}\left(-\mathrm{grad}p^w + \rho^w\boldsymbol{g}\right), \\ \rho_g C_p^g\boldsymbol{v}^g &= n\rho^g C_p^g\frac{k^{rg}\boldsymbol{k}\rho^{gw}}{\mu^g}\left(-\mathrm{grad}p^g + \rho^g\boldsymbol{g}\right)\,. \end{aligned} \tag{12}$$

In the previous relationships, $\boldsymbol{v}^w$ is the advective velocity of water, $\boldsymbol{v}^g$ is the advective velocity of gas, C_p is the specific heat capacity of the system while C_p^s, C_p^w and C_p^g are the heat capacities of the particular species of the mixture. Finally, linear momentum balance equation of the multiphase medium

$$\mathrm{div}\left(\boldsymbol{\sigma}^{\mathrm{eff}} - \alpha(S_w p^w + S_g p^g)\boldsymbol{m}^{\mathrm{T}}\right) + \rho \boldsymbol{g} = 0\,, \tag{13}$$

where $\boldsymbol{\sigma}^{\mathrm{eff}}$ is the effective stress tensor and $\boldsymbol{m}^T = (1,1,1,0,0,0)$ is the auxiliary vector.

The balance equations have to be completed by initial and boundary conditions. The initial conditions specify the field of displacements, pore water and gas pressures, and temperature at time $t = 0$ in the form

$$\boldsymbol{u} = \boldsymbol{u}_0, \qquad p^w = p_0^w, \qquad p^g = p_0^g, \qquad T = T_0, \qquad \text{in } \Omega \text{ and on } \Gamma, \tag{14}$$

where $\boldsymbol{u}_0$, p_0^w, p_0^g and T_0 are known functions. Ω is the domain of interest and Γ its boundary. The domain boundary Γ is split into parts Γ_u, Γ_T, Γ_w, Γ_g with prescribed values of displacements, temperature, water pressure and gas pressure and parts Γ_t, Γ_{qg}, Γ_{qw}, Γ_{qT} with prescribed densities of fluxes, i.e. surface traction, flux of gas, flux of water and heat flux. The boundary conditions for displacements and stresses in the mechanical part are completed by Dirichlet boundary conditions with prescribed values

$$\begin{aligned}
\boldsymbol{u} &= \boldsymbol{u}_0, && \text{on } \Gamma_u,\\
\boldsymbol{n}\boldsymbol{\sigma} &= \boldsymbol{t}, && \text{on } \Gamma_t,\\
p^w &= \overline{p}^w, && \text{on } \Gamma_w,\\
p^g &= \overline{p}^g, && \text{on } \Gamma_g,\\
T &= \overline{T}, && \text{on } \Gamma_T,
\end{aligned} \tag{15}$$

and the flux boundary conditions for fluxes of gas, water, and heat

$$\begin{aligned}
q_n^{ga} &= \left[\frac{k^{rg}\boldsymbol{k}\rho^{ga}}{\mu^g}(-\mathrm{grad}p^g + \rho^g \boldsymbol{g}) + \rho^g \frac{M_a M_w}{M_g^2}\boldsymbol{D}_g \mathrm{grad}\left(\frac{p^{gw}}{p^g}\right)\right]\cdot \boldsymbol{n}, && \text{on } \Gamma_{qg},\\
q_n^w &+ q_n^{gw} + \beta(\rho^{gw} - \rho_\infty^{gw}) = \left[\frac{k^{rw}\boldsymbol{k}\rho^w}{\mu^w}(-\mathrm{grad}p^w + \rho^w \boldsymbol{g})\right]\cdot \boldsymbol{n}\\
&+ \left[\frac{k^{rg}\boldsymbol{k}\rho^{gw}}{\mu^g}(-\mathrm{grad}p^g + \rho^g \boldsymbol{g})\right]\cdot \boldsymbol{n} - \left[\rho^g \frac{M_a M_w}{M_g^2}\boldsymbol{D}_g \mathrm{grad}\left(\frac{p^{gw}}{p^g}\right)\right]\cdot \boldsymbol{n}, && \text{on } \Gamma_{qw},\\
q_n^T &+ \beta_T(T - T_{ext}) + e\sigma_0(T^4 - T_\infty^4) = [-\boldsymbol{\lambda}_{\mathrm{eff}}\mathrm{grad}T]\cdot \boldsymbol{n}\\
&+ \left[\frac{k^{rw}\boldsymbol{k}\rho^w}{\mu^w}(-\mathrm{grad}p^w + \rho^w \boldsymbol{g})\,\Delta H_{\mathrm{vap}}\right]\cdot \boldsymbol{n}, && \text{on } \Gamma_{qT}.
\end{aligned} \tag{16}$$

where q_n^{ga}, q_n^w, q_n^{gw} and q_n^T are fluxes in the normal direction to the boundary Γ.

Application of the Galerkin method to the balance equations (8-13) leads to the governing equations in weak form. Discretisation of unknown functions in the space has to satisfy inf-sup condition. The primary variables are expressed by their nodal values and shape functions. In the standard Galerkin procedure, the weight functions are replaced by the corresponding shape functions. The detailed derivation of the final system of equations can be found in [4]. The final non-linear system of ordinary differential equations can be expressed in the matrix form

$$
\begin{aligned}
&\begin{pmatrix} \boldsymbol{K}_{uu} & \boldsymbol{K}_{uw} & \boldsymbol{K}_{ug} & \boldsymbol{K}_{uT} \\ \boldsymbol{K}_{wu} & \boldsymbol{K}_{ww} & \boldsymbol{K}_{wg} & \boldsymbol{K}_{wT} \\ \boldsymbol{K}_{gu} & \boldsymbol{K}_{gw} & \boldsymbol{K}_{gg} & \boldsymbol{K}_{gT} \\ \boldsymbol{K}_{Tu} & \boldsymbol{K}_{Tw} & \boldsymbol{K}_{Tg} & \boldsymbol{K}_{TT} \end{pmatrix} \begin{pmatrix} \boldsymbol{d}_u \\ \boldsymbol{d}_w \\ \boldsymbol{d}_g \\ \boldsymbol{d}_T \end{pmatrix} + \\
&+ \begin{pmatrix} \boldsymbol{C}_{uu} & \boldsymbol{C}_{uw} & \boldsymbol{C}_{ug} & \boldsymbol{C}_{uT} \\ \boldsymbol{C}_{wu} & \boldsymbol{C}_{ww} & \boldsymbol{C}_{wg} & \boldsymbol{C}_{wT} \\ \boldsymbol{C}_{gu} & \boldsymbol{C}_{gw} & \boldsymbol{C}_{gg} & \boldsymbol{C}_{gT} \\ \boldsymbol{C}_{Tu} & \boldsymbol{C}_{Tw} & \boldsymbol{C}_{Tg} & \boldsymbol{C}_{TT} \end{pmatrix} \begin{pmatrix} \dot{\boldsymbol{d}}_u \\ \dot{\boldsymbol{d}}_w \\ \dot{\boldsymbol{d}}_g \\ \dot{\boldsymbol{d}}_T \end{pmatrix} = \begin{pmatrix} \boldsymbol{f}_{ext} \\ \boldsymbol{f}_w \\ \boldsymbol{f}_g \\ \boldsymbol{f}_T \end{pmatrix} ,
\end{aligned}
\tag{17}
$$

where the subscript u denotes the displacements, and the subscripts w, g, T represent pore water pressure, p^w, pore gas pressure, p^g, and temperature, T. The vectors $\boldsymbol{d}_u$, $\boldsymbol{d}_w$, $\boldsymbol{d}_g$, and $\boldsymbol{d}_T$ stand for their unknown nodal variables, and the vectors $\boldsymbol{f}_{ext}$, $\boldsymbol{f}_w$, $\boldsymbol{f}_g$, and $\boldsymbol{f}_T$ denote nodal forces and fluxes prescribed in boundary conditions in (16). The matrices $\boldsymbol{K}$ with subscripts represent the generally non-linear non-symmetric stiffness, conductivity, permeability, and coupling matrices, and $\boldsymbol{C}$ denotes the capacity and coupling matrix.

The system of equations (17) could be written in the compact form

$$\boldsymbol{C}\dot{\boldsymbol{d}} + \boldsymbol{K}\boldsymbol{d} = \boldsymbol{f} \ . \tag{18}$$

The generalized trapezoidal rule is based on the assumption, that the vector of nodal values $\boldsymbol{d}$ evaluated at time instant $i+1$ is in the form

$$\boldsymbol{d}_{i+1} = \boldsymbol{d}_i + \Delta t \boldsymbol{v}_{i+\alpha} \ , \tag{19}$$

where the vector $\boldsymbol{v}_{i+\alpha}$ has form

$$\boldsymbol{v}_{i+\alpha} = (1-\alpha)\dot{\boldsymbol{d}}_i + \alpha\dot{\boldsymbol{d}}_{i+1} \ . \tag{20}$$

Substitution of expressions (19) and (20) to the equation (18) results in

$$\left(\boldsymbol{C} + \Delta t \alpha \boldsymbol{K}\right)\dot{\boldsymbol{d}}_{i+1} = \boldsymbol{f}_{i+1} - \boldsymbol{K}\left(\boldsymbol{d}_i + \Delta t(1-\alpha)\dot{\boldsymbol{d}}_i\right) \ , \tag{21}$$

which is a system of algebraic equations. If the system (18) is nonlinear, the system (21) is also nonlinear. The non-linear system (21) is solved using Newton's iterative method. This means that, in order to achieve acceptable residuals in the non-linear system, a system of linear algebraic equations is solved repeatedly. Furthermore, the non-linear system (21) is solved at every time step, which, when there are a large number of unknowns, places enormous demands on computational power.

4 Numerical example

In order to assess the safety of a deep geological repository for radioactive waste, it is necessary to carry out a whole series of numerical simulations, including a description of the behaviour of the excavation damage zone. This paper describes the coupled thermo-hydro-mechanical problem in the vicinity of a single disposal borehole. The situation is depicted in Figure 1. The red colour represents the waste disposal package,

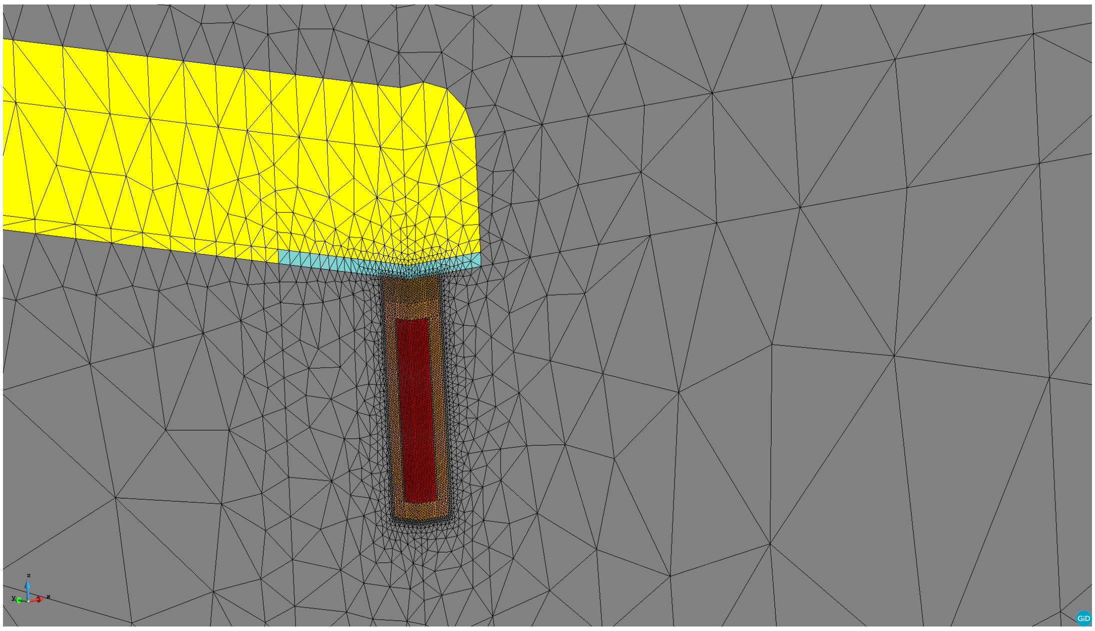

Figure 1: Scheme of domain solved and finite element mesh.

the dark orange colour represents the bentonite buffer, the yellow colour represents the access tunnel, which will ultimately also be filled with bentonite, and the grey colour represents the rock mass. The diameter of the waste disposal package is assumed approximately 90 cm, its length is about 6 m, and due to the influence of the disposal package, it is necessary to model a relatively large surrounding area of the borehole. It results in 189,337 nodes and 1,072,055 finite tetrahedral elements. The material parameters of the rock mass are: density 2,650 kg/m^3, specific heat capacity 790 J/K/kg, heat conductivity 2.5 J/m^2/s/K. The material parameters of the bentonite are: density from 1,400 to 1,700 kg/m^3, specific heat capacity 1,350-1,700 J/kg/K, heat conductivity 0.3-0.75 J/s/m^2/K. Initial temperature is assumed 11 ^{o}C. Figure 2 shows the expected evolution of the power output of a waste disposal package in time. Figure 3 shows distribution of temperature and water saturation which will be the values that become the boundary conditions for the excavation damage zone.

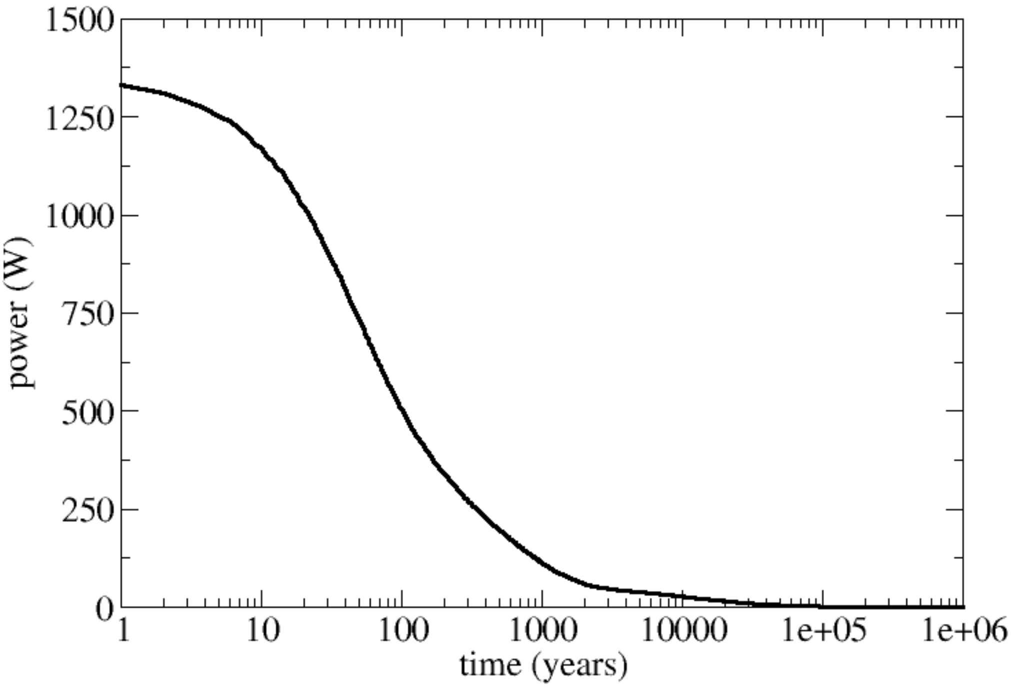

Figure 2: Expected power of a waste disposal package.

5 Conclusion

Published simulations of a coupled thermo-hydro-mechanical problem indicate the boundary conditions for transport problems within the excavation damage zone in a rock mass. A high-quality bentonite buffer minimises the risk of radioactive substances spreading beyond the radioactive waste repository. The transport properties of the excavation damage zone only come into play when the saturation level and the temperature front approach the damage zone. The thickness of the damage zone is of the order of tens of centimetres, so transport processes are briefly accelerated; however, upon reaching the virtually undamaged rock mass, everything slows down dramatically and further behaviour is characterised by the properties of undamaged rock.

Acknowledgements

The financial support provided by the GAČR grant No. 26-20457S is gratefully acknowledged.

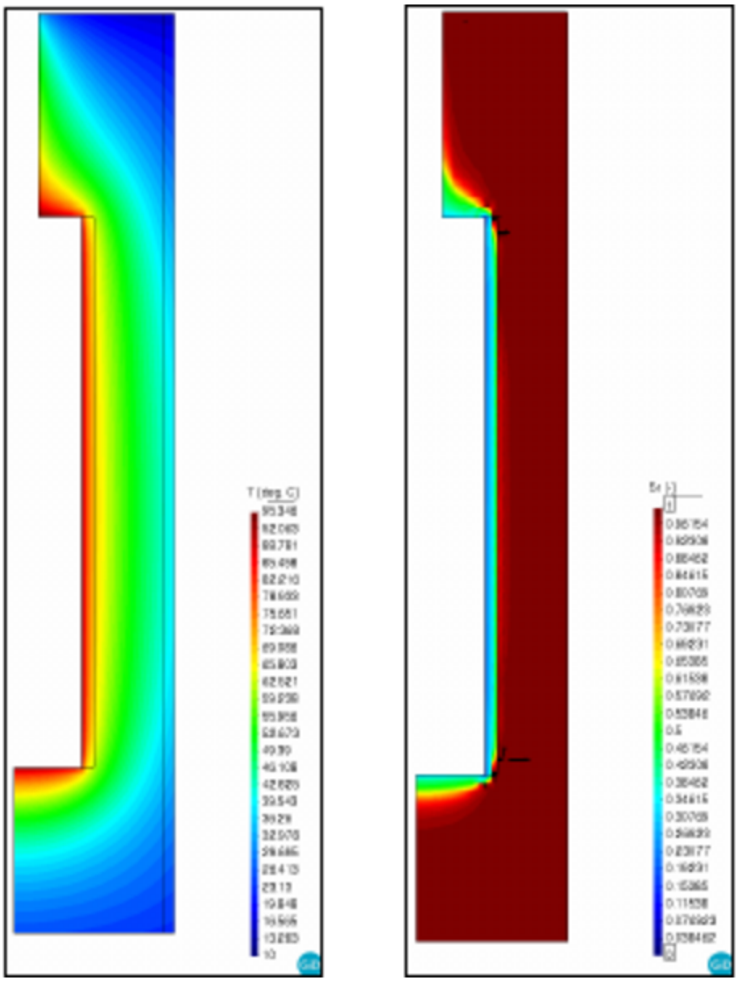

Figure 3: Distribution of temperature and degree of saturation.

References

[1] D. Mašín, “Predictive modelling of clay behaviour using a double structure framework”, Computers and Geotechnics, 40, 93-104, 2012.

[2] D. Mašín, “Coupled thermo-hydro-mechanical double structure model for expansive soils”, Acta Geotechnica, 12, 89-108, 2017.

[3] E. Simo, T. Helfer, T. Gerasimov, C. Lehmann, D. Naumov, T. Krejčí, T. Koudelka, J. Kruis, T. Nagel, D. Mašín, “Wrapper-based integration of a thermo-hydro-mechanical hypoplastic bentonite model in OpenGeoSys via MFront”, Advances in Engineering Software, 215, 104106, 2026.

[4] R.W. Lewis, B.A. Schrefler, The Finite Element Method in the Static and Dynamic Deformation and Consolidation of Porous Media, John Wiley & Sons, Chichester, England, 2000, 2nd edition, ISBN 0 471 92809 7.

[5] F. Claret, N. I. Prasianakis, A. Baksay, D. Lukin, G. Pepin, E. Ahusborde, B. Amaziane, G. Bátor, D. Becker, A. Bednár, M. Béreš, S. Bérešová, Z. Böthi, V.

Brendler, K. Brenner, J. Březina, F. Chave, S. V. Churakov, M. Hokr, D. Horák, D. Jacques, F. Jankovský, C. Kazymyrenko, T. Koudelka, T. Kovács, T. Krejčí, J. Kruis, E. Laloy, J. Landa, T. Ligurský, T. Lipping, C. López-Vázquez, R. Masson, J. C. L. Meeussen, M. Mollaali, A. Mon, L. Montenegro, B. Pisani, J. Poonoosamy, S. I. Pospiech, Z. Saâdi, J. Samper, A. C. Samper-Pilar, G. Scaringi, S. Sysala, K. Yoshioka, Y. Yang, M. Zuna, O. Kolditz, "EURAD state-of-the-art report: development and improvement of numerical methods and tools for modeling coupled processes in the field of nuclear waste disposal", Frontiers in Nuclear Engineering, 2024, 10.3389/fnuen.2024.1437714